THE EFFECTS OF ANNEALING ON MICROSTRUCTURE AND TENSILE PROPERTIES OF COLD DRAWN STEEL WIRE

Nur Alyani Nazirah Mohammad Rafix[1], Nor Akmal Fadil[1,2,*], Astuty Amrin[3], Abdollah Bahador[3], Wan Fahmin Faiz Wan Ali[1,2] and Suhaimi Salleh[4]

[1]Faculty of Mechanical Engineering, Universiti Teknologi Malaysia, 81300 UTM Johor Bahru, Malaysia
[2]Materials Research and Consultancy Group, Universiti Teknologi Malaysia, 81310 Johor Bahru, Johor, Malaysia
[3]Razak Faculty of Technology and Informatics, UTM Kuala Lumpur, 54100 Kuala Lumpur
[4]Kisswire, No. 33, Jalan Senyum, Kampung Wadihana 80300 Johor Bahru Johor

*norakmal@utm.my

Abstract. Annealing is a process that could improve the tensile properties of material while eliminating internal residual stress created during cold drawing process. This study aimed to investigate the effect of annealing temperature and soaking time on cold-drawn steel wire in terms of microstructural changes and mechanical properties. The effects of annealing temperature and soaking time were investigated using tensile test, X-ray diffractometer (XRD) and field emission scanning electron microscope (FESEM). The tensile strength decreased from 2030.48 MPa (untreated) to 1984.81, 1988.04 and 1978.15 MPa when annealed at 425 ºC for 0.5, 5, 10 minutes of soaking times, respectively. As the annealing temperature increased to 475 ºC, the tensile strength further decreased to 1855.90, 1864.35 and 1774.39 MPa, for the same soaking times respectively. Obviously, prolonged soaking time at higher annealing temperature will only reduce the tensile strength up until 2.5%. The reduction of tensile strength for the annealed samples was attributed to the age softening due to the break-up of the lamellar cementite structure and the recovery of lamellar ferrite. This accompany with stress reduction which has been evidenced by analysing XRD peak patterns. The XRD peak shows that increasing in annealing temperature and soaking time resulted in the decrease of full width at half maximum (FWHM) values, indicating the reduction in the residual stress. Overall, this study demonstrated that controlled annealing at 425 ºC and the soaking time as low as 0.5 minute is sufficient to effectively reduce the residual stress caused by cold drawing process, while maintaining materials strength.

Keywords: High carbon steel wire, cold drawing, annealing, residual stress, age softening, cementite dissolution

Article Info

Received 3rd March 2023
Accepted 6th April 2023
Published 1st May 2023

ISSN: 1823-7010, eISSN: 2600-7444

Introduction

Steel wire rope is commonly used in the heavy industry such as suspension bridge, cable car, elevator, and cranes due to its outstanding mechanical properties. The wire rope is made of a galvanized high carbon steel wire that is drawn from a single wire before being twisted into wire strands with specific design configuration. Cold drawn steel wire is produced by reducing the diameter of the original wire to its desired diameter. Steel wire rope in engineering applications is required to have high strength and high corrosion resistance to withstand and operate at not only high temperatures, but also high loading conditions. According to previous research, cold drawing process could improve the tensile strength of the steel wire from 1200 MPa to 2300 MPa at drawing strain of $\varepsilon = 2.4$ [1]. Several research have studied the influence of annealing process of cold-drawn steel wire on its mechanical properties [2-4]. Haslan (2013) has found that the microstructure of cold-drawn steel wire is influenced by the annealing temperature [5] which subsequently affect the mechanical properties of drawn wire due to the age softening and age hardening phenomena.

Although the drawing process improves the strength of the steel wire, however, it may develop unnecessary residual stresses in wire [6]. The development of residual stress will then reduce the fatigue life of the material [7]. The residual stress present in a sample would increase steadily with drawing strain [7-8]. The mechanical properties of drawn wire can be improved by the refinement of interlamellar spacing, the addition of carbon content and alloying elements, and the increment of dislocation density [9]. However, the higher the strength of the materials, it will reduce the ductility and multiplying the amount of residual stress.

The friction at the die-specimen interphase during the drawing process develops dislocation and the amount of inhomogeneity due to plastic deformation which will generate residual stresses on the drawn steel wire [8]. Even after the external loads have been removed, the stresses remained in the wire to achieve the state of equilibrium [8]. Withers et al. has elaborated that residual stresses from applied stress would cause an unexpected failure such as stress corrosion cracking (SCC) due to the combined stress of residual stress and applied stress [7]. In fact, the residual stress also will become an internal source of energy for diffusion at atomic level, that associated with the aging phenomena [10]. X-ray diffraction analysis were commonly used to study the effect of residual stress in a steel wire [10-11]. Annealing has been introduced in cold drawn steel wire to reduce the residual stress from drawing process [9]. Annealing process will increase the partial dissolution of cementite structure due to the change's behavior of dislocation density and its direct relationship with residual stress of cold drawn wire.

Residual stress can be generated as a result of deformation during the wire drawing process. To attain wires with optimal mechanical properties, it is crucial to carefully select appropriate heat treatment parameters. This study investigates the impact of microstructural alterations prior to and post the annealing process on residual stress and tensile properties of the drawn wires.

Materials and Methods

Sample Preparation

The cold-drawn wire was acquired from Kiswire Sdn Bhd consisting of Fe-0.92%C-0.25%Si-0.67%Mn (wt.%). The received wires were drawn from 11 mm to 5.1 mm (ε = 0.77). The annealing process was conducted on drawn wire at temperature of 425 ºC and 475 ºC, the soaking time was maintained at 0.5, 5 and 10 minutes, respectively using Cole-Parmer stable temperature muffle furnace followed by furnace cool.

Metallography Study

Field emission scanning electron microscope (FESEM SU8020, Hitachi) was employed to examine the microstructural changes before and after the annealing process. Annealed samples were cut in longitudinal sections followed by hot mounting process. The samples were ground using SiC-based paper from 200 grits to 2000 grits and polished using 1 µm alumina suspension to obtain a mirror-like surface. The polished samples were etched with 2% Nital etchant and were air dried. The average of five cementite layers at three different locations was measured as inter-lamellar spacing as shown in Equation 1 [12].

$$\Delta L = \frac{\left(\frac{H1}{5}\right)+\left(\frac{H2}{5}\right)+\left(\frac{H3}{5}\right)}{3} \quad (1)$$

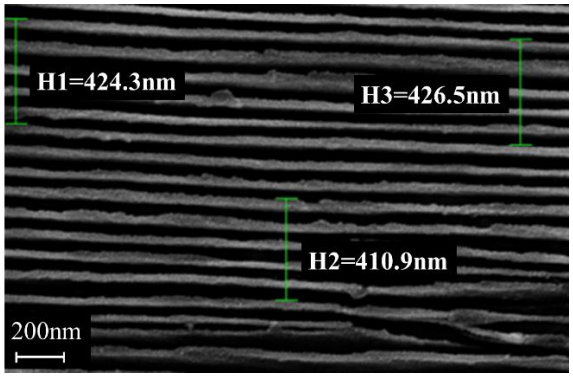

Figure 1: Inter-lamellar spacing measurement using FESEM for untreated sample

Tensile Test

The mechanical properties of the annealed samples for different annealing temperature and soaking time were determined and compared with the untreated samples using Instron universal testing machine following ASTM D3039 Standard. The sample was cut to 200 mm length prior to anneal at various annealing temperature and soaking time.

X-Ray Diffraction (XRD)

XRD analysis was conducted to determine the phases present and changes in full width at half maximum (FWHM) of XRD peaks for the annealed wires. CuKα radiation (RIGAKU; λ = 0.1548 nm) with a step width of 0.01º and scanning rate of 3º/min were employed. The scanning window was between 20º and 100º of the Bragg's angle (2Θ). The

peak analysis was conducted at lattice plane of (110) and (211). The XRD analysis were conducted using X'pert Highscore software to determine the FWHM values of the XRD peaks.

Results and Discussion

Effect of Annealing on Microstructure

Figures 2 and 3 show the FESEM micrographs of untreated and annealed samples at different annealing conditions. Figure 2 shows that the untreated steel wire consists of uniform high planarity of lamellar shape. Annealed wire at 425 ºC for 0.5 minute of soaking time shows the break-up of lamellar cementite structure as shown in Figure 2(b). The break-up structure of a lamellar cementite layer is indicated by the changes in the planarity of the lamellar layers. This phenomena shows that the age softening process has started to occur as early as 0.5 minute of soaking time at 425 ºC [9]. By increasing the soaking time to 10 minutes as shown in Figure 2(c), the lamellar cementite shape has changed becoming even more non-planar which indicates that the degree of age softening process has increased. The results show that the age softening process will start to develop even during short soaking time (0.5 minute) due to the breaks of lamellar cementite structure and the high intensity of carbon atoms in lamellar ferrite in cold drawn steel wires. This will then cause the spheroidization and reprecipitation of cementite particles, while the recovery of ferrite occurred during the rising of annealing temperature from the room temperature [13].

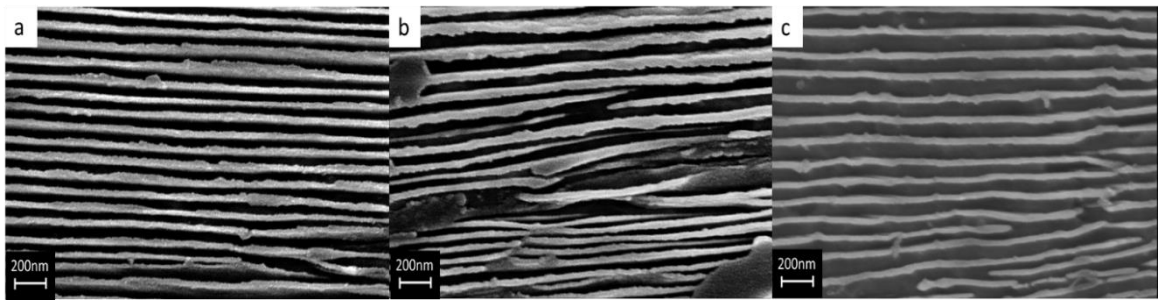

Figure 2: The FESEM micrographs of (a) untreated sample (b) annealed at 425 ºC for 0.5 minute and (c) annealed at 425 ºC for 10 minutes

However, when the samples were annealed at higher temperature of 475 ºC, the changes in lamellar structure are more noticeable regardless of the soaking time (Figure 3). The interdiffusion effect of lamellar cementite in Figure 3(b) was easily observed which indicates that the phenomena were governed by age softening. As the soaking time prolonged to 10 minutes, greater changes in pearlite structure can be clearly observed in Figure 3(c) as compared to 0.5 minute in Figure 3(b). When annealed at a higher annealing temperature and soaking time, it will increase the degree of break-up of lamellar cementite instead of the decomposition of lamellar cementite [9]. As observed in Figure 3(c), at some areas, the shape of the lamellar cementite started to form globular structure. This is due to the interdiffusion in lamellar structure [7,9,14]. It is clearly shown that the annealing temperature of 425 ºC and 475 ºC was able to initiate the changes in the microstructure when annealed only for 0.5 minutes. The interdiffusion in lamellar cementite and the tendency to develop the cementite particles were more prominent when the annealing period was increased to 10 minutes.

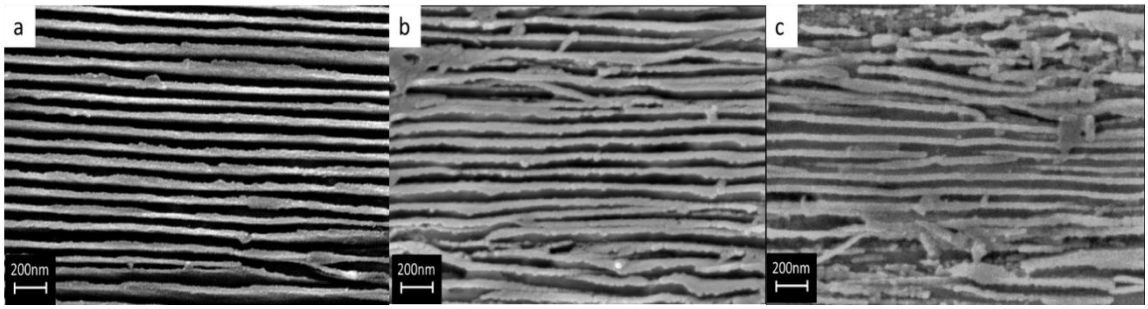

Figure 3: The FESEM micrographs of (a) untreated sample (b) annealed at 475 ºC for 0.5 minute and (c) annealed at 475 ºC for 10 minutes

Figure 4 illustrates the inter-lamellar spacing of the untreated and annealed steel wire at 425 ºC and 475 ºC for 0.5 and 10 minutes. Inter-lamellar spacing of annealed steel wire was observed to increase with soaking time from 84.11 to 111.41 and 115.15 nm for 0.5 and 10 minutes at annealing temperature of 425 ºC. However, at annealing temperature of 475 ºC, the interlamellar spacing decreases from 84.11 to 81.50 nm when annealed for 0.5 minutes and slightly increase to 84.7 nm when soaking time prolonged to 10 minutes. When the soaking time is prolonged to 10 minutes, the inter-lamellar spacing continues to increase slightly as the break-up of the lamellar structure is more prominent. This result is well-corresponded to the observed microstructure in Figure 3(c) where the dissolution of carbon atoms in lamellar cementite increased. Since there are no obvious changes in the inter-lamellar spacing at different annealing parameter, the effect of annealing parameter on inter-lamellar spacing can be neglected.

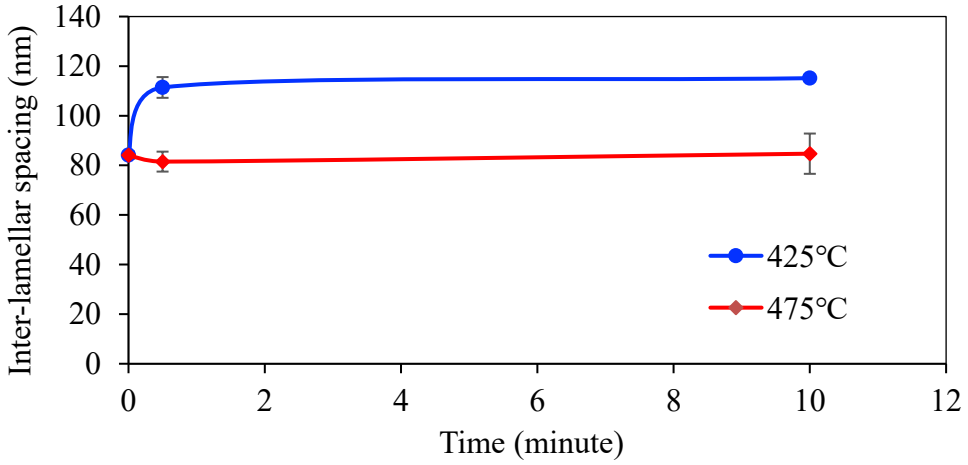

Figure 4: Inter-lamellar spacing for annealed steel wire at different soaking time and temperature

Tensile Properties

The tensile strength versus soaking time curve for annealed steel wire at different annealing temperatures are shown in Figure 5. The tensile strength decreased from 2030.48 to 1984.81, 1988.04 and 1978.15 MPa when annealed at 425 ºC for (0.5, 5, 10) minutes, while at 475 ºC, it has further decreased to 1855.90, 1864.35 and 1774.39 MPa. Annealing at 425 ºC and 475 ºC for 0.5 minutes shows a reduction in tensile strength due to age softening process. This result is corresponding to the microstructure findings in Figures 2 and 3 where

the interdiffusion in lamellar cementite is noticeable. A smaller reduction of tensile strength is observed when annealed at 425 ºC suggesting that the age softening happened on the annealed samples, but less as compared to 475 ºC. Moreover, when increasing the soaking time up to 10 minutes, the annealed samples demonstrate continuous reduction in tensile strength. Higher degree of tensile strength reduction at temperature of 475 ºC compared to 425 ºC is due to the higher releasing of residual stress in this sample [15]. Several research has reported that increasing the annealing temperature and time will reduce the tensile strength [2,4,16]. From the tensile test analysis, it can be concluded that annealing process could maintain its tensile strength with minimal reduction (about 2.5%) after annealing process, despite the reduction of the residual stress in the samples.

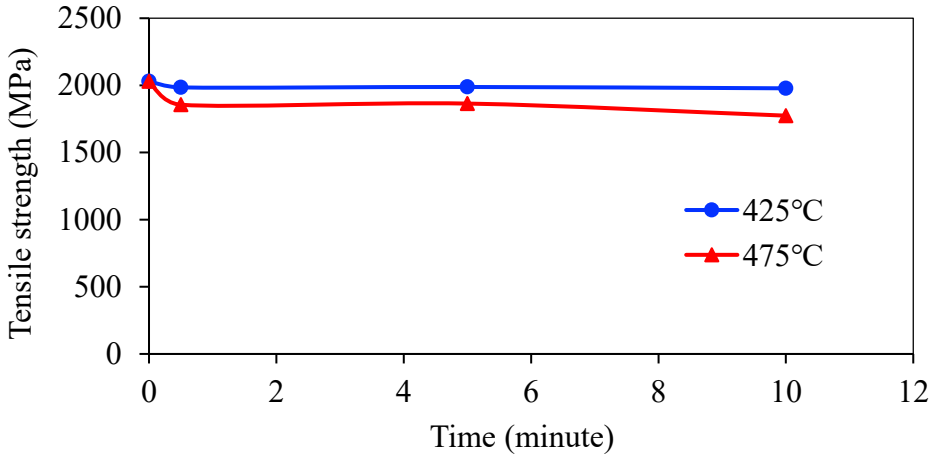

Figure 5: Tensile strength at different annealing temperature (425 ºC and 475 ºC) until 10 minutes of soaking time

XRD Analysis

Figure 6 illustrates the XRD patterns of drawn wire annealed at 425 ºC and 475 ºC for 0.5 minutes and 10 minutes, respectively. The peaks are indexed and matched to the body-centered cubic (BCC) structure of carbon steel. The first and second strongest peaks in Figure 6 is located at 2Θ=44.60º and 2Θ=82.20º corresponding to the (110) and (211) planes of the carbon steel reference XRD pattern [16].

The influence of annealing temperature on the structural properties and residual stress of the steel wires were determined from the shift in peaks. Figure 7 shows the high magnification of reflected peaks from (110) and (211) planes for each sample and the reference XRD pattern of iron-carbon. Table 1 and 2 show the XRD peak data for plane (110) and (211) for untreated and treated samples. A slight shift of the peaks to higher angle at plane (110) and (211) were observed for all the samples when annealed for 0.5 minutes and slightly decrease to lower angle at plane (110) when soaking time is prolonged to 10 minutes.

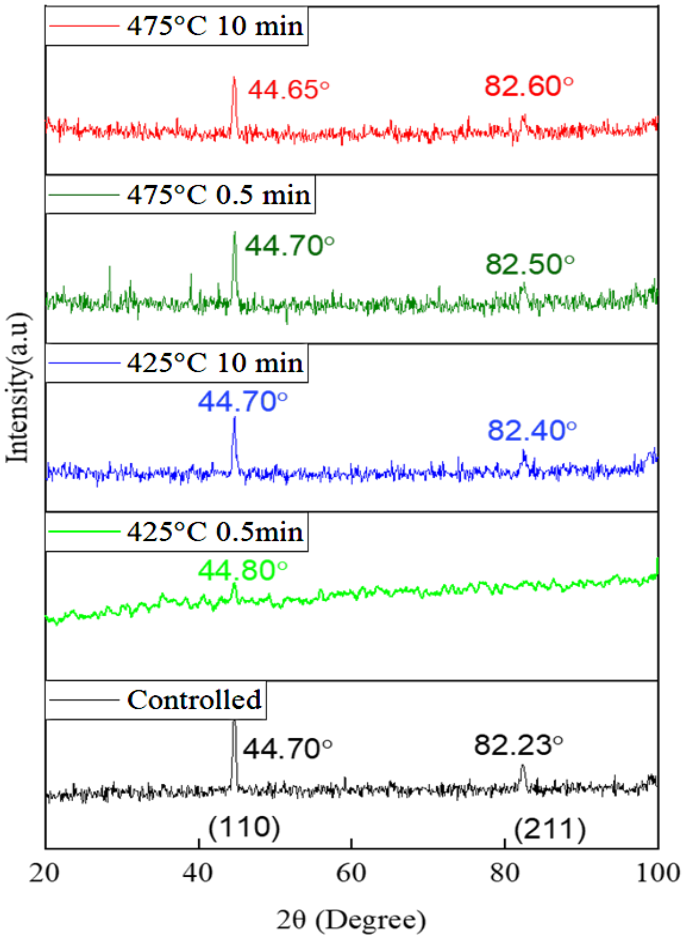

Figure 6: XRD patterns of high carbon steel wire (0.92 wt.%C) at different annealing temperature and soaking time

The difference in the peaks angle when annealed compared to the untreated sample shows a significant difference. When annealed at annealing temperature of 425 ºC for 0.5 minute, the peaks are shifted from 44.70º to 44.80º. This higher peak angle is due to the release of residual stress during age softening as discussed in the previous section. Furthermore, when annealed time further to 10 minutes, the peak angle seems to slightly decrease to 44.70º. This trend could also be seen when annealed at 475 ºC. This is due to less residual stress release when continuously annealed at longer time. An experiment conducted by previous research has showed that different annealing parameter will effect on the peak angle which correlates with residual stress [17]. However, the results in this research were not able to correlate with the XRD shift theory as reported in the previous research. Peak broadness changes also can be related to changes in residual stress of cold worked carbon steel when annealed at specific annealing time and temperature [18-19].

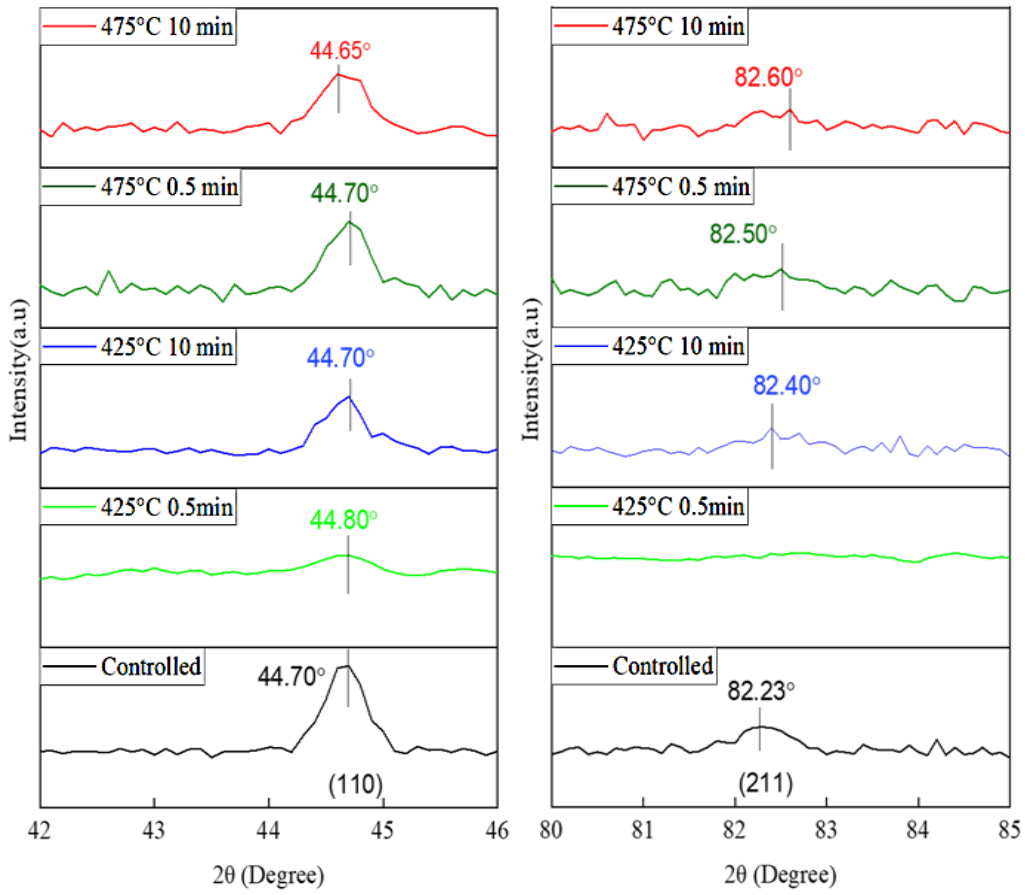

Figure 7: XRD peak analysis for plane (110) and (211) for control and annealed samples at 425 ºC and 475 ºC for 0.5 and 10 minutes

Table 1: XRD peak data for plane (110) for untreated and treated samples

Annealing temperature (ºC)	Annealing time (minutes)	Bragg's Angle, 2Θ (Degree)	d (Å)	FWHM
untreated sample		44.70	2.0262	0.513
425	0.5	44.80	2.0214	0.352
	10	44.70	2.0262	0.481
475	0.5	44.70	2.0262	0.498
	10	44.65	2.0278	0.632

Table 2: XRD peak data for plane (211) for untreated and treated samples

Annealing temperature (ºC)	Annealing time (minutes)	Bragg's Angle, 2Θ (Degree)	d (Å)	FWHM
untreated sample		82.23	1.1714	0.638
425	0.5	no peak detected		
	10	82.40	1.1694	0.499
475	0.5	82.50	1.1683	0.521
	10	82.60	1.1671	0.421

Figures 8 and 9 show the effects of annealing temperature and soaking time on FWHM at plane (110) and plane (211), respectively. Previous research by Fu et al. [18], stated that the FWHM analysis could be used for the residual stress analysis. Peak will broaden when the crystal size is reduced or vice versa, or when there is a defect in the crystal lattice [19]. Analysis at plane (110) shows that the reduction on FWHM value from 0.513 to 0.352 and 0.498 occur when annealed for 0.5 minute of soaking time at 425 ºC and 475 ºC respectively but increases to 0.481 and 0.632 when soaking time prolonged to 10 minutes. This result contradicts with the statement that higher soaking time will promote the reduction of FWHM which was related to the release of residual stress [18].

However, the XRD peak analysis for the plane (211) shows a consistent result with previous research [18-19], where the FWHM decreases when annealed for 10 minutes at 425 ºC. Since no peak were detected at plane (211) for sample annealed at 425 ºC for 0.5 minutes, no specific data could be used for the FWHM analysis. Similar trends also shown by the samples annealed at 475 ºC for 0.5 and 10 minutes when the XRD peaks analysis is conducted at plane (211). The FWHM values decrease significantly with soaking time from 0.638 to 0.521 and 0.421. The FWHM value is the lowest when annealed for 10 minutes because the cementite dissolution is increased when soaking time is increased as shown in Figures 2(c) and 3(c). This will then increase the reduction of micro-strain at higher soaking time and temperature [18]. This result corresponds to the theory that annealing process would reduce the residual stress on cold drawn steel wire [9]. Furthermore, the analysis at plane (211) clearly shows a significant results which provides higher reliability since the higher angle of XRD peak is more sensitive to the changes of external stimuli [20].

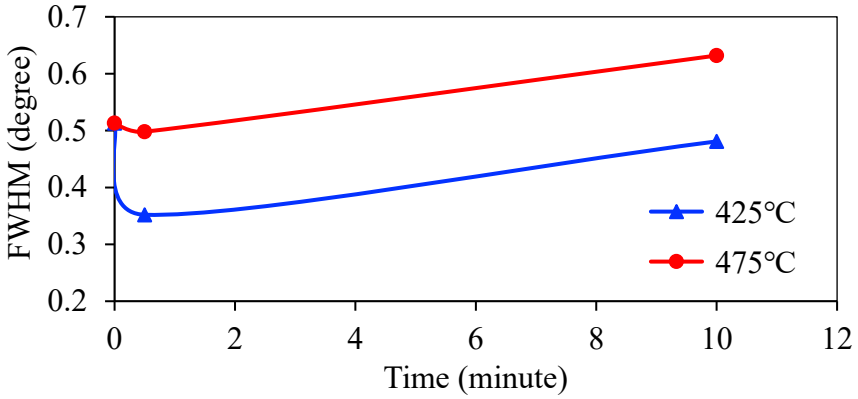

Figure 8: Effect of annealing temperature and soaking time on FWHM at plane (110)

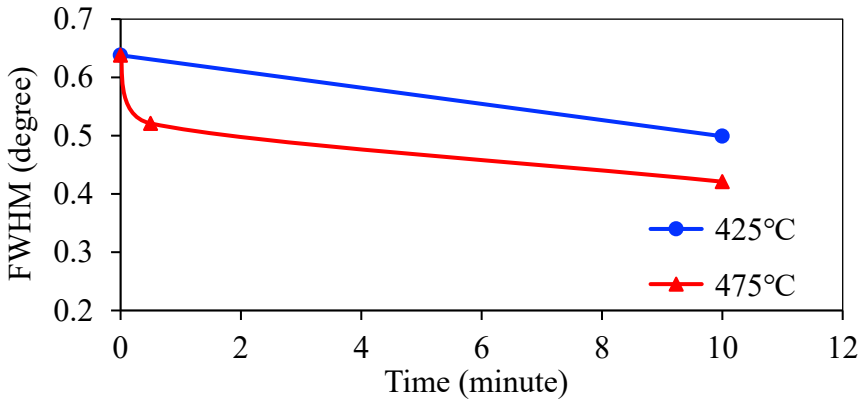

Figure 9: Effect of annealing temperature and soaking time on FWHM at plane (211)

Conclusions

The effects of the annealing parameters on microstructure and tensile properties of drawn steel wire with 0.92%C were investigated. It is clearly shown that the annealing temperature of 425 ºC and 475 ºC was able to initiate the age softening process when annealed only for 0.5 minute of soaking time as indicated by the break-up lamellar cementite structure from the FESEM micrographs. The break-up of lamellar cementite structure was more prominent when the soaking time was increased to 10 minutes. Inter-lamellar spacing of annealed steel wire was observed to increase with soaking time of 0.5 and 10 minutes. The tensile strength decreases from 2030.48 (untreated) to 1984.81, 1988.04 and 1978.15 MPa when annealed at 425 ºC for (0.5, 5, 10) minutes. Furthermore, tensile strength decreases to 1855.90, 1864.35 and 1774.39 MPa when annealed at 475 ºC for (0.5, 5, 10) minutes. From the tensile test analysis, it can be concluded that annealing process could maintain its tensile strength with minimal reduction after annealing process while reducing the internal residual stress. FWHM XRD peak analysis at plane (110) and (211) shows that the FWHM value decrease significantly with annealing temperature and soaking time due to the reduction in the residual stress of cold drawn steel wire.

Acknowledgements

This work was financially supported by the Universiti Teknologi Malaysia under the grant scheme of UTM R&D Fund (R.J130000.7751.4J510) and UTM ER (Q.J130000.3851.19J39).

Author Contributions

All authors contributed toward data analysis, drafting and critically revising the paper and agree to be accountable for all aspects of the work.

Disclosure of Conflict of Interest

The authors have no disclosures to declare.

Compliance with Ethical Standards

The work is compliant with ethical standards

References

[1] Jung, J. Y., An, K. S., Park, P. Y. & Nam, W. J. (2020). Effects of Wire Drawing and Annealing Conditions on Torsional Ductility of Cold Drawn and Annealed Hyper-Eutectoid Steel Wires. *Journal of the Metals (Basel)*. 10(8), 1–11.

[2] Gerstein, G., Niimberger, F., Dudzinski, W., Grygier, D., Schaper, M. & Milenin, A. (2014). Structural Evolution of Thin Lamellar Cementite During Cold Drawing of Eutectoid

Steels. In Proceedings of the International Conference on Technology of Plasticity (ICTP'2014), Japan, 19-24 Oct 2014.

[3] Hono, K., Ohnuma, M., Murayama, M., Nishida, S., Yoshie, A. & Takahashi, T. (2001). Cementite Decomposition in Heavily Drawn Pearlite Steel Wire. *Journal of the Scripta Materialia*. 46(2), 175–177.

[4] Haddi, A., Imad, A. & Vega, G. (2011). Analysis of Temperature and Speed Effects on The Drawing Stress for Improving the Wire Drawing Process. *Journal of Materials and Design*. 32(8), 4310–4315.

[5] Haslan, N. H. (2013). Effects of Heat Treatment on the Microstructures and Electrochemical Behavior of Stainless Steel. (M. Eng. Thesis, Universiti Teknologi Malaysia, Malaysia) pp. 20-80.

[6] He, S., Bael, A. V., Li, S. Y., Houtte, P. V., Mei, F. & Sarban, A. (2003). Residual Stress Determination in Cold Drawn Steel Wire by FEM Simulation and X-Ray Diffraction. *Journal of Materials Science and Engineering.* 346(1–2), 101–107.

[7] Withers, P. J. (2007). Residual Stress and its Role in Failure. *Journal of Reports on Progress in Physics*. 70(12), 2211–2264.

[8] Tacq, J. (2015). Residual And Internal Stress Development Resulting From Plastic Deformation Of Multi-Phase Alloys. (Doctoral Dissertation, Katholieke Universiteit Leuven, Belgium) pp. 65-161.

[9] Lee, J. W., Lee, J. C., Lee, Y. S., Park, K. T. & Nam, W. J. (2009). Effects of Post-Deformation Annealing Conditions on the Behavior of Lamellar Cementite and the Occurrence of Delamination in Cold Drawn Steel Wires. *Journal of the Material Processing Technology*. 209(12–13), 5300–5304.

[10] Fadil, N. A., Yusof, S. Z., Bakar, T. A., Ghazali, H., Mat, M. A., Osman, A. S. & Ourdjini, A. (2021). Tin Whiskers' Behavior Under Stress Load and the Mitigation Method for Immersion Tin Surface Finish. *Journals of Materials.* 14(22), 6817.

[11] Osman, A. (2004). Residual Stress Measurement Using X-Ray Diffraction. (M. Sci. Thesis, Texas A&M University, United States) pp. 20-76.

[12] Hu, X., Houtte, P. V., Liebeherr, M., Walentek, A., Seefeldt, M. & Vandekinderen, H. (2006). Modeling Work Hardening of Pearlitic Steels by Phenomenological and Taylor-Type Micromechanical Models. *Journal of Acta Materialia*. 54(4), 1029-1040.

[13] Jung, J. Y., An, K. S., Park, P. Y. & Nam., W. J. (2021). Correlation Between Microstructures and Ductility Parameters of Cold Drawn Hyper-Eutectoid Steel Wires with Different Drawing Strains and Post-Deformation Annealing Conditions. *Journal of Metals (Basel)*. 11(2), 1–16.

[14] Neves, F. O., Oliviera, T. L. L., Braga, D. U. & Silva, A. S. C. (2014). Influence of Heat Treatment on Residual Stress in Cold-Forged Parts. *Journal of Advance in Materials Science and Engineering*. 2014, 1-7.

[15] Zhang, X., Mcmurtrey, M., Wang, L. & O'brien, R. (2020). Evolution of Microstructure, Residual Stress, and Tensile Properties of Additively Manufactured Stainless Steel Under Heat Treatments. *Journal of the Minerals, Metals & Materials Society*. 72(12), 4167–4177.

[16] Swanson, E. H., Morris, M, C. & Evans, E. H. (1966). *Standard X-Ray Diffraction Powder Patterns*. 4th edition (United States Department of Commerce National Bureau of Standards) pp. 1-10.

[17] Shen, J. N., Zeng, Y. B., Xu, M. H., Zhu, L. H., Liua, B. L. & Guoa, H. (2019). Effects of Annealing Parameters on Residual Stress and Piezoelectric Performance of ZnO Thin Films Studied by X-Ray Diffraction and Atomic Force Microscopy. *Journal of Applied Crystallography*. 52(5), 951–959.

[18] Fu, P., Chu, R., Xu, Z., Ding, G. & Jiang, C. (2018). Relation of Hardness with FWHM and Residual Stress of GCr15 Steel After Shot Peening. *Journal of Applied Surface Science*. 431, 165–169.

[19] Ungár, T. (2004). Microstructural Parameters from X-Ray Diffraction Peak Broadening. *Journal of Scripta Materialia*. 51(8), 777–781.

[20] Luo, Q. & Yang, S. (2017). Uncertainty of the X-Ray Diffraction (XRD) sin2 Ψ Technique in Measuring Residual Stresses of Physical Vapor Deposition (Pvd) Hard Coatings. *Journal of Coatings*. 7(8), 128.